General Disclaimer

One or more of the Following Statements may affect this Document

- This document has been reproduced from the best copy furnished by the organizational source. It is being released in the interest of making available as much information as possible.

- This document may contain data, which exceeds the sheet parameters. It was furnished in this condition by the organizational source and is the best copy available.

- This document may contain tone-on-tone or color graphs, charts and/or pictures, which have been reproduced in black and white.

- This document is paginated as submitted by the original source.

- Portions of this document are not fully legible due to the historical nature of some of the material. However, it is the best reproduction available from the original submission.

Produced by the NASA Center for Aerospace Information (CASI)

N O T I C E

THIS DOCUMENT HAS BEEN REPRODUCED FROM
MICROFICHE. ALTHOUGH IT IS RECOGNIZED THAT
CERTAIN PORTIONS ARE ILLEGIBLE, IT IS BEING RELEASED
IN THE INTEREST OF MAKING AVAILABLE AS MUCH
INFORMATION AS POSSIBLE

NASA

Technical Memorandum 82114

Interplanetary Magnetic
Clouds at 1 AU

L. W. Klein and L. F. Burlaga

APRIL 1981

INTERPLANETARY MAGNETIC CLOUDS AT 1 AU

by

L. W. Klein
Computer Sciences Corporation
8728 Colesville Road
Silver Spring, MD 20910

and

L. F. Burlaga
NASA/Goddard Space Flight Center
Laboratory for Extraterrestrial Physics
Greenbelt, MD 20771

ABSTRACT

Magnetic clouds are defined as regions with a radial dimension $\gtrsim 0.25$ AU (at 1 AU) in which the magnetic field strength is high and the magnetic field direction changes appreciably by means of rotation of one component of $\underset{\sim}{B}$ nearly parallel to a plane. The magnetic field geometry in such a magnetic cloud is consistent with that of a magnetic loop, but it cannot be determined uniquely. Forty-five clouds were identified in inter-planetary data obtained near earth between 1967 and 1978; at least one cloud passed the earth every three months. Three classes of clouds were identified, corresponding to the association of a cloud with a shock, a stream interface, or a CME. There are approximately equal numbers of clouds in each class, and the field and plasma parameters in each class are similar suggesting that the three types of clouds might be different manifestations of a single phenomenon (e.g., a coronal transient). Inter-face-associated clouds may have been swept up by corotating streams. Shock-associated clouds move faster than the other two types, which are basically slow flows. The magnetic pressure inside the clouds is higher than the ion pressure and the sum is higher than the pressure of the material outside of the cloud. This implies that the magnetic clouds were expanding even at 1 AU, and the average expansion speed is estimated to be of the order of half the ambient Alfvén speed.

1. Introduction

The ejection of plasma and magnetic fields from active regions on the sun was proposed by Morrison (1954), who called such ejecta "magnetic clouds". Gold (1955) proposed that a magnetic cloud might be preceded by a shock wave. The dynamics of a magnetic cloud were analyzed in a remarkable but forgotten paper by Parker (1957). The topology of the magnetic field in a magnetic cloud was discussed by Cocconi et al. (1958) and Gold (1959, 1962), who suggested that the magnetic field lines form an "elongated tongue" or "magnetic bottle" with field lines rooted at both ends in the sun, and by Piddington (1958), who suggested that the magnetic field lines might "reconnect" to form a magnetic "bubble" consisting of closed field lines. Numerous observations of magnetic fields associated with transient post-shock flows have been published, but little is known about the three-dimensional configuration and dynamics of the magnetic field in magnetic clouds.

A number of authors have suggested the existence of magnetic "loops" behind shocks on the basis of indirect measurements such as electron temperature (Montgomery et al., 1974), proton temperature (Gosling et al., 1973), energetic particles (e.g., Palmer et al., 1978), and superthermal electrons (Bame et al., 1981), but without considering the magnetic field measurements. Schatten et al. (1968) presented some evidence for a magnetic loop in the IMP magnetic field measurements; Bobrov (1979) observed a systematic variation of one component of B behind a shock which he identified with a magnetic loop; and Podovkin et al. (1977, 1979) offered statistical evidence for magnetic loops based on interplanetary and solar magnetic field measurements.

Burlaga and Klein (1980) and Burlaga et al. (1981) analyzed the magnetic field configurations behind three shocks and found a systematic variation in the direction of B. Specifically, they found that only two components of B changed (in a minimum variance coordinate system) as a cloud moved past the spacecraft. We shall call such configurations "magnetic clouds". The condition of planarity places a strong constraint on the geometry of the lines of force in a magnetic cloud. Nevertheless,

it does not provide enough information to determine the configuration
uniquely from observations at just one spacecraft, since information on the
third dimension is not available. Burlaga et al. (1981) used data from 5
spacecraft separated in the radial and azimuthal directions to examine the
structure of one magnetic cloud. King et al. (1981) applied the method of
Burlaga and Klein (1980) to the analysis of one stream observed near earth.
The aim of this paper is to survey statistical characteristics of many
magnetic clouds, using data from one spacecraft (actually a series of
isolated spacecraft).

2. Selection and Classification of Magnetic Clouds

With hour averages of the magnetic field data from 1967 to 1978
compiled by King (1977, 1979) (primarily from GSFC magnetometers on the IMP
spacecraft), we selected magnetic clouds using the following operational
definition: 1) the duration is approximately one day, corresponding to a
characteristic dimension $\sim$ 0.25 AU; 2) the magnetic field direction changes
nearly monotonically from large southern (northern) directions to large
northern (southern) directions; 3) the magnetic field vectors are nearly
parallel to a plane; and 4) the magnetic field strength is higher than
average. First a selection was made subjectively from King's plots of $B(t)$
using conditions 1, 2, and 4, and the additional constraint that there be
nearly complete measurements of $B(t)$, $V(t)$ (speed), $n(t)$ (density), and
$T(t)$ (proton temperature) for each magnetic cloud. This procedure
identified 70 events, which provide a good statistical sample but does not
include all magnetic clouds that passed the spacecraft. We then analyze
$B(t)$ in each of these events using a minimum variance analysis in order to
select the events which satisfied condition 3 above, i.e., events for which
the ratio of the intermediate to minimum eigenvalues is greater than two
$(\lambda_2/\lambda_3 > 2)$. For each magnetic cloud, we carried out the minimum variance
analysis (Sonnerup and Cahill, 1967) using several non-overlapping
intervals inside the cloud and using different boundaries, and we selected
only those events for which a consistent set of results was obtained. In
this way we obtained a set of 45 magnetic clouds which are the subject of
the rest of this paper.

The operational definition of a magnetic cloud given above is based on the characteristics of the magnetic clouds discussed by Burlaga and Klein (1980) and by Burlaga et al. (1981), which happened to follow shocks. However, our definition does not require the presence of a shock or any other discontinuity. Magnetic clouds do not always follow shocks, although some may do so.

The 45 magnetic clouds (hereafter simply called clouds) that we selected fall into one of the following groups:

1) cloud preceded by a shock

2) cloud followed by a stream interface (see Belcher and Davis, 1971; Burlaga, 1974; and Gosling et al., 1978)

3) cloud associated with a CME (a region in which the plasma temperature is anomalously low and the magnetic field strength is enhanced--see Burlaga et al. (1981).

This classification is similar to that used by Burlaga and King (1979) for enhancements in magnetic field strength. The remainder of this section is given to a discussion of examples of clouds in each class.

A cloud following a shock is shown in Figure 1. The shock is identified by the simultaneous increase in F, V, n and T_p. The magnetic cloud is identified with the $\hat{\ } $ 33 hr interval beginning 9 hrs after the shock, in which $|\theta|$ is relatively large (magnetic field directed out of the ecliptic) and the field strength is high. The results of the minimum variance analysis are shown in the panels on the right of Figure 1. The change in $\underset{\wedge}{B}$ takes place in a plane, and there is no significant component of $\underset{\wedge}{B}$ normal to this plane. The minimum variance direction is determined very accurately $(\lambda_2/\lambda_3 = 9.9)$, and it is given in solar ecliptic coordinates by $\phi_n = 195°$, $\theta_n = 24°$. The velocity, density and temperature profiles in Figure 1 show that the magnetic cloud was embedded in a low-density, relatively cold stream. Such material has been identified as flare ejecta which drive a shock (for example, see Hundhausen, 1972; Burlaga et al., 1980, and references therein). Thus, it is tempting to identify the magnetic cloud as a loop carried away from the sun by ejecta from a flare or some other transient.

A cloud associated with a stream interface is shown in Figure 2. The interface is identified with the simultaneous increase in T, increase in V and decrease in n at a time when F is maximum. The magnetic cloud is identified with the 24-hr interval in which the magnetic field changes from a northern direction to a southern direction and the magnetic field strength is high. The results of the minimum variance analysis on the right of Figure 1 show that in the cloud $\underset{\sim}{B}(t)$ changes direction by rotating in a plane $(\lambda_2/\lambda_3 = 16.6)$, with essentially no component of $\underset{\sim}{B}$ normal to that plane. The minimum variance direction (normal to the plane of rotation) is nearly radial, $\phi_n = 182°$ and $\theta_n = -1°$. The plasma parameters following the cloud are typical of those in corotating streams, and we may assume that the peak in F is due to the stream interaction. The cloud itself, however, precedes the stream, although its trailing end may be affected by the compression wave generated by the stream interaction. In the cloud, the temperature is low, the magnetic field strength is high, and the speed is near average; these are characteristics of a CME. Thus, the cloud is a flow system distinct from the corotating stream but adjacent to it. It is possible that the cloud was injected some distance ahead of the stream but has been overtaken by the stream before it reached 1 AU. In this case, there is a sector boundary between the cloud and stream. Some of the "thick" sector boundaries observed by Klein and Burlaga (1980) might include magnetic clouds; for example, the April, 1973 event in their Figure 5. In general, if a magnetic cloud lies adjacent to a thin sector boundary, the definition that Klein and Burlaga used for a sector boundary will classify the configuration as a thick sector boundary. The problem arises because of the high inclinations of the fields in a magnetic cloud.

A magnetic cloud associated with a CME but not with an interface or shock is illustrated in Figure 3. The CME is recognized as a region of low temperature and high field strength. The boundaries of the cloud are chosen on the basis of the temperature and field strength profiles. The minimum variance analysis shows one component of $\underset{\sim}{B}(t)$ in the cloud (B_z) is constant while the other rotates in the B_x-B_y plane. Thus again only two components of the field are changing, but now the magnetic field lines are helical, rather than confined to a series of parallel planes. Another

example of a magnetic cloud which is associated with a CME but not a shock or interface is shown in Figure 4. In this case the cloud is well-defined by the variations in $F(t)$ and $\theta(t)$. In the front half of the cloud the temperature is low and F is high, indicating that it is a CME; the cloud seems to be larger than the CME. The minimum variance analysis shows that $\underset{\sim}{B}$ rotates close to a plane, with possibly a small component of $\underset{\sim}{B}$ along the minimum variance direction. This magnetic cloud precedes a sector boundary.

3. Statistical Properties of Plane Magnetic Clouds

The 45 magnetic clouds that we selected fall into the three classes described in the preceding section as follows: 13 clouds following shocks (Table 1a); 16 clouds preceding stream interfaces and interaction regions (Table 1b); and 16 clouds associated with CMEs (Table 1c). Any given magnetic cloud is described by the minimum variance direction (θ_n, ϕ_n), the magnetic field profile (especially $F(t)$ and $\theta(t)$), and plasma parameters ($V(t)$, $n(t)$ and $T(t)$). To study the dynamics of magnetic clouds, it is instructive to consider the dynamical pressure (ρV^2), the sum of magnetic and proton thermal pressures ($B^2/(8\pi) + nkT_p$) and the ratio $\beta = nkT_p/(B^2/8\pi)$. This section examines the behavior of these parameters for each of the three classes of magnetic clouds.

The distributions of minimum variance directions for each of the three classes of magnetic clouds are shown in Figure 5. Consider first the distributions of the component of the minimum variance direction in the ecliptic plane, whose direction is given by ϕ_n. For the clouds associated with CMEs, ϕ_n is relatively close to the radial direction ($\pm 30°$) and symmetric about it. For the clouds associated with shocks, ϕ_n scatters more about the radial direction, but again it is roughly symmetric about it. However, for clouds associated with interaction regions, there is a distinct tendency for ϕ_n to be orthogonal to the spiral direction. Since interaction regions associated with stream interfaces tend to be large-scale features aligned along the spiral direction and preceding fast streams, this result suggests that clouds associated with interfaces are swept up and ordered by corotating streams.

The distributions of θ_n, the elevation of the minimum variance direction with respect to the ecliptic plane, are also shown in Figure 5. For all three classes of clouds, θ_n is close to the ecliptic ($\pm 30°$). There is, however, a tendency for the minimum variance direction to avoid the ecliptic plane in clouds associated with shocks and CME's. It is possible that there are "magnetic clouds" in which there is little or no variation in θ_n but a large variation in ϕ_n. Such clouds were not considered in this study because they might be confused with narrow sectors. The minimum variance directions for such clouds would be nearly normal to the ecliptic plane. Thus the ϕ_n distribution shown in Figure 5 might not describe "magnetic clouds" defined more generally.

In order to compare the profiles $F(t)$ and $\theta(t)$ for the three classes of clouds, we produced a superposed epoch plot for each class from the individual profiles $F_i(t)$, $\theta_i(t)$ of events in that class. For example, for the 16 clouds preceding interfaces we arranged the profiles such that the front boundaries were aligned at $t = 0$ and we then computed running 6-hr averages of $F_i(t)$ and $|\theta_i(t)|$. The results are shown in Figure 6. The curves are the running means and the error bars are the RMS deviations divided by the square root of the number of events for successive 6-hr intervals. For this discussion we take the duration of a cloud to be 24 hours, and the behavior of $F(t)$ and $|\theta(t)|$ in the clouds is indicated by the shaded regions in Figure 6.

As expected from our selection criteria, $F(t)$ and $|\theta(t)|$ are high inside the clouds relative to the values outside. Significantly, the maximum strength of B is the same for all three classes of clouds, ~ 12 nT. For clouds associated with CME's, the enhanced field strengths are confined to the clouds. For clouds associated with shocks, the field strength is enhanced somewhat for several hours ahead of the cloud, probably because of shock compression. The field strength and $|\theta(t)|$ are enhanced for more than 24 hours after the passage of the front boundaries of the shock-associated clouds suggesting that these clouds are larger than CME-associated clouds. For clouds associated with interfaces, the field strength is not enhanced ahead of the cloud, but it is enhanced behind the cloud owing to the interaction region which follows the cloud.

Superposed-epoch plots of V(t), n(t) end $T_p(t)$ for the three classes of clouds are shown in Figure 7. Consider the clouds associated with CMEs. The speed of these clouds is essentially that of the quiet solar wind; they are at rest relative to the slow solar wind in which they are embedded. The density in those clouds is somewhat higher than average, $\sim 11/cm^3$, while the temperature is low, $\sim 4 \times 10^4$ °K. Now consider the interface-associated clouds. They are followed by fast streams of hot, low-density plasma typical of the corotating streams that are related to interfaces. Near the rear boundary the temperature, density and speed are enhanced owing to the compression wave from the interaction region. Thus the cloud characteristics are represented by the first ~ 12 hours of data after $T = 0$. One finds low speeds (~ 400 km/s), low temperatures (to $\sim 4 \times 10^4$ °K) and densities higher than average ($\sim 14/cm^3$). Note that the clouds which precede interfaces closely resemble those associated with CMEs, if one disregards the effects of the compression waves on the former. This suggests that the two classes of clouds actually represent only one type of object. In this view both classes of clouds are cold regions with strong fields rotating in two dimensions. Those associated with interfaces presumably originated near coronal holes which produced streams that follow interfaces, and they were subsequently swept up by the streams.

The plasma parameter profiles for the shock-associated clouds resemble those for the two classes of clouds described above in that the temperature falls to low values ($\sim 5 \times 10^4$ °K) and the density is $\sim 10/cm^3$. However, the speeds of these clouds ($\sim 450/$km/s) are higher than those of the CME and interface-associated clouds. The shock-associated clouds appear to be moving faster than the ambient solar wind ahead whereas the other types of clouds are not. Possibly this relative motion is driving the shock. This suggests that all three classes of magnetic clouds might represent essentially the same type of physical structure, the shock-associated clouds differing from the other two classes primarily in that they are moving relative to the flow ahead of them. Of course, the shock itself produces some differences in the density and temperature profiles ahead of the clouds (see Figure 7) but these are not fundamental characteristics of the clouds.

Let us restate the hypotheses arrived at in the preceding paragraphs. It was suggested that there is predominantly just one type of magnetic cloud, a cold region with strong spatially ordered fields represented most clearly by the clouds associated with CMEs. Some slow clouds happen to be overtaken by fast, corotating streams and are thus associated with interfaces and modified somewhat by a compression wave from the stream interaction. Other clouds are advancing relative to the ambient solar wind, and the relative motion at some point along the trajectory is fast enough to produce a shock wave; these clouds are thus classified as shock-associated clouds.

This picture is supported by the behavior of the dynamical quantities β = $nkT_p/(B^2/8\pi)$, P^2 = $(B^2/8\pi)$ + nkT_p, and M = ρV^2 shown in the superposed epoch plots in Figure 8. For all three classes of clouds, β is low: $\sim$ 0.2 ± 0.1 in CME's, $\sim$ 0.3 ± 0.2 behind shocks, and $\sim$ 0.5 ± 0.2 ahead of interfaces. The pressure profiles are particularly interesting. In all three types of clouds, the proton pressure is 2 to 3 times the ambient value ($\sim$ 6 x 10^{-10} dynes/cm^2), which means that the clouds are probably not in equilibrium with the ambient solar wind. For example, the pressure in clouds associated with CME's is much higher than that ahead of or behind the clouds, so they will tend to expand, even though they have no radial bulk motion relative to the surrounding solar wind. The expansion is primarily normal to $\underset{\sim}{B}$, since β << 1. This expansion will tend to cool the plasma, and may be a cause of the low temperatures observed in these clouds. These clouds are clearly not equilibrium structures such as those discussed by Rosenberg and Coleman (1980) and Akasofu (1979), and they are unlike interaction regions in which the pressure gradient is balanced by a gradient in momentum flux (Burlaga and Ogilvie, 1970). The situation is similar in the other two classes of clouds, except that there is an additional pressure peak ahead of the shock-associated clouds owing to shock compression, and there is a pressure peak behind the interface-associated clouds owing to the stream interaction wave.

4. Expansion of Magnetic Clouds and a Possible Relation to Coronal Transients

White light observations of the solar corona have revealed transients (coronal mass ejection events) moving away from the sun with speed of the order of 400 km/s at 5 R_0, and there is evidence that many have the form of loops which expand as the transients move outward (Anzer, 1978; Anzer and Pneuman, 1981; Pneuman, 1980, 1981; Mouschovias and Poland, 1978; MacQueen, 1980). Since they move faster than the escape speed, and since there is no evidence that they return to the sun, one expects to see these transients in the solar wind. However, only one transient has been related to an interplanetary event (Gosling et al., 1974) and in that case only the interplanentary shock was observed, not the transient ejecta. It is reasonable to ask whether the magnetic clouds that we have described are related to coronal mass ejection events. Two approaches are possible: direct correlation between magnetic clouds and solar features corresponding to coronal transients, and a comparison of the physical properties of magnetic clouds with those of coronal transients. Let us consider the second approach.

The speeds of the magnetic clouds at 1 AU are approximately 400-450 km/s. This is close to the average speed of mass ejection events reported by Rust et al. (1979), as 474 km/s, and it is within the range of speeds reported by Poland et al. (1980). The mass of a magnetic cloud can be estimated from the observed density ($\rho_1 \sim 10/cm^3$) and size (L $\sim$ 0.25 AU). The average diameter of the magnetic cloud is greater than its average measured length, since a spacecraft does not always intercept a cloud along its largest dimension; we shall take the diameter to be $\sim$ 1.5L $\sim$ 0.4 AU, corresponding to random interception of spheres. Thus, the mass of a magnetic cloud is of the order of $(10/cm^3)$ $(4\pi/3)$ $(0.2 \times 1.5 \times 10^{13} cm)^3$ $(1.7 \times 10^{-24} g)$ = $2 \times 10^{15} g$. This is comparable to the mass of a coronal transient: Hildner (1977) reported an average mass of $6 \times 10^{15} g$ and Poland et al. (1980) reported an average of $8.5 \times 10^{15} g$.

The average magnetic field strength in a magnetic cloud at 1 AU is $\sim$ 12nT and the field is highly inclined with respect to the ecliptic.

Thus, using flux conservation and the observed size of a cloud at 1 AU, we estimate that the field strength in a magnetic cloud at 2 R_o is $\sim$ 12 (0.2 x 215 R_o/1R_o)^2 $\sim$ 0.2 G. Dulk et al. (1976) estimated that B $\sim$ 1G in one transient at 2 R_o, which is nearly of the same order of magnitude as our estimate for magnetic clouds.

We identified 70 clouds in $\sim$ 11 years of data. Correcting for the data gaps, this implies the order of 0.5 to 1 cloud/month. Transients are observed near the sun at a rate of $\sim$ 1-3/day (Hildner, 1977; Poland et al., 1980). The probability of intercepting a transient is of the order of (0.25/2π) = 0.04. Hence one expects to see them at 1 AU at a rate of $\sim$ 1/25 days to $\sim$ 3/25 days, which is of the same order of magnitude as the rate at which clouds are observed.

We conclude that the observed mass, field strength and occurrence rate of magnetic clouds is consistent with the corresponding numbers for coronal mass ejection events, to order of magnitude. Thus, our observations do not preclude the possibility that magnetic clouds are coronal mass ejection events. Clearly it would be worthwhile to search for a direct association between a coronal transient and a magnetic cloud. This is not possible with data from earth-orbiting spacecraft because transients are observed only near the limbs while the plasma that is seen comes from near central meridian.

We noted that the observed "size" of a magnetic cloud is typically $\sim$ 0.25 AU and we inferred a radius of $\sim$ 0.2 AU for a spherical cloud at 1 AU. This obviously implies that the radius of cloud increases considerably as it moves from the sun to 1 AU and we may ask if the required expansion rate is reasonable. Suppose that beyond $\sim$ 5 R_o the cloud expands at a speed equal to the local ambient Alfvén speed, $V_{A1}(r)$ $\sim$ $B(r)/(4\pi \rho(r))^{1/2}$. Taking $E = B_1(r_1/r)^2 (1 + r/r_1)^2)^{1/2}$ and $V_{A1}/V \sim 0.1$, one finds that the radius of a cloud at 1 AU is $\sim$ 0.4 AU. This is nearly twice the observed radius, implying that the actual expansion speed is of the order of $V_{A1}/2$, which is a reasonable rate. This rate implies that the relative flow owing to expansion is subsonic, hence ambient plasma can accommodate the expansion of the cloud without the formation of a shock.

Thus, the motion of a cloud in interplanetary space may be relatively
simple when its center of mass moves subsonically with respect to the
ambient flow. The theoretical study of such subsonic flows in the solar
wind has been neglected.

5. Summary

We have investigated the statistical characteristics of magnetic
clouds observed in the interplanetary medium near earth. A magnetic cloud
is defined here as a structure which moves past a spacecraft in
approximately one day, and in which the magnetic field strength is higher
than average and the magnetic field direction changes nearly monotonically
from large southern (northern) to large northern (southern) directions. In
particular we identified and described 45 magnetic clouds in which one
component of $\underset{\sim}{B}$ changes direction by rotating parallel to a plane while the
component of $\underset{\sim}{B}$ normal to that plane is either constant or zero. Such
clouds are not uncommon, being observed near earth at the rate of at least
one every three months, averaged over a solar cycle.

We identified and described three classes of magnetic clouds: 1) cloud
preceded by a shock; 2) cloud followed by a stream interface, and 3) cloud
associated with a CME. There were approximately equal numbers of clouds in
each class. The minimum variance directions for clouds associated with
CME's and for those associated with shocks scattered about the radial
direction as one would expect for a transient "projectile". By contrast,
the minimum variance directions in clouds associated with interfaces tend
to be normal to the spiral direction, suggesting that those clouds are
aligned along the spiral by virtue of their association with streams that
follow interfaces.

In superposed epoch plots, the maximum field strength is found to be
approximately the same for each class of clouds, viz. $\hat{\sim}$ 12 nT. Similarly,
the temperatures are low ($\sim 4 \times 10^{4}$ °K) and the densities are somewhat high
(10-14/cc) in all three types of clouds. These results suggest that the
three types of clouds might be simply different manifestations of a single
phenomenon. The clouds associated with shocks move with respect to the

ambient flow, and this motion might be responsible for the shock. The other two classes of clouds have no motion with respect to the plasma ahead. Interface-associated clouds might simply be CME's that have been swept up by streams.

In all three classes of clouds, the pressure is higher than the ambient pressure, and the magnetic field provides the dominant contribution, at least in the center of the cloud. Thus, the clouds are not stationary; they must be expanding. An expansion rate of approximately half the ambient Alfvén speed would account for the observed size of the clouds. Such motion might also be a cause of the low temperature observed in magnetic clouds. Expansion would imply relatively high magnetic field strengths and densities near the sun.

The observed physical characteristics of magnetic clouds and their rate of occurrence suggests that many or all of the clouds might be related to coronal mass eject events (solar transients) that have been observed in white light data. Further studies are needed to evaluate this hypothesis.

REFERENCES

Akasofu, S-I., Radial deformation of the solar current sheet as a cause of geomagnetic storms, Planetary Space Sci., 27, 1055, 1979.

Anzer, U., Can coronal loop transients be driven magnetically?, Solar Phys., 57, 111, 1978.

Anzer, U., and G. W. Pneuman, Magnetic reconnection and coronal transients, submitted to Solar Phys., 1981.

Bame, S. J., J. R. Asbridge, W. C. Feldman, J. T. Gosling, and R. D. Zwickl, Bi-directional streaming of solar wind electrons > 80 eV: ISEE evidence for a closed-field structure within the driver gas of an interplanetary shock, Geophys. Res. Lett., in press, 1981.

Belcher, J., and L. Davis, Jr., Large-amplitude Alfvén waves in the interplanetary medium, 2, J. Geophys. Res., 76, 3534, 1971.

Bobrov, M. S., Magnetic classification of solar wind streams, Planetary Space Sci., 27, 1461, 1979.

Burlaga, L. F. Interplanetary stream interfaces, J. Geophys. Res., 79, 3717, 1974.

Burlaga, L. F., and J. H. King, Intense interplanetary magnetic fields observed by geocentric spacecraft during 1963-1975, J. Geophys. Res., 84, 6633, 1979.

Burlaga, L. F., L. W. Klein, Magnetic clouds in the solar wind, NASA/GSFC TM 80668, 1980.

Burlaga, L., R. Lepping, R. Weber, T. Armstrong, C. Goodrich, J. Sullivan, D. Gurnett, P. Kellogg, E. Keppler, F. Mariani, F. Neubauer, H. Rosenbauer, and R. Schwenn, Interplanetary particles and fields, November 22 – December 6, 1977: Helios, Voyager and IMP observations between 0.6 AU and 1.6 AU, J. Geophys. Res., 85, 2227, 1980.

Burlaga, L., E. Sittler, F. Mariani, and R. Schwenn, Magnetic loop behind an interplanetary shock: Voyager, Helios and IMP-8 observations, NASA/GSFC TM 82086, J. Geophys. Res. (submitted), 1981.

Cocconi, G., T. Gold, K. Greisen, S. Hayakawa, and P. Morrison, The cosmic ray flare effect, Nuovo Cimento, 8, 161, 1958.

Dulk, G. A., S. F. Smerd, R. M. MacQueen, J. T. Gosling, A. Magun, R. T. Stewart, K. V. Sheridan, R. D. Robinson, and S. Jacques, Solar Phys. 49, 369, 1976.

Gold, T., Contributions to discussion of gas dynamics of cosmic clouds, p. 103, North-Holland Publishing Co., Amsterdam, 1955.

Gold, T., Plasma and magnetic fields in the solar system, J. Geophys. Res., 64, 1665, 1959.

Gold, T., Magnetic storms, Space Sci. Rev., 1, 100, 1962.

Gosling, J. T., V. Pizzo, S. J. Bame, Anamolously low proton temperatures in the solar wind following interplanetary shock waves: Evidence for magnetic bottles?, J. Geophys. Res., 78, 2001, 1973.

Gosling, J. T., J. R. Asbridge, S. J. Bame, and W. C. Feldman, Solar wind stream interfaces, J. Geophys. Res., 83, 1401, 1978.

Gosling, J. T., E. Hildner, R. M. MacQueen, R. H. Munro, A. I. Poland, and C. L. Ross, Mass ejections from the sun: A view from Skylab, J. Geophys. Res., 79, 4581, 1974.

Hildner, E., In studies of traveling interplanetary phenomena, (ed. M. A. Shea et al.), p. 3, Dordrecht, D. Reidel, 1977.

Hundhausen, A. J., Coronal Expansion in the Solar Wind, p. 192, Springer-Verlag, NY, 1972.

King, J. H., Interplanetary Medium Data Book, GSFC/NSSDC/WCD-A R&S, 77-04, 1977.

King, J. H., Interplanetary Medium Data Book, Supplement 1, NSSDC/WDC-A-R&S, 79-04, 1979.

King, J. H., R. P. Lepping, and J. D. Sullivan, On the complex state of the interplanetary medium of July 28-29, 1977, J. Geophys. Res., submitted, 1981.

Klein, L. W., and L. F. Burlaga, Interplanetary sector boundaries: 1971-1973, J. Geophys. Res., 85, 2269, 1980.

MacQueen, R. M., Coronal transients: A summary, Phil. Trans. R. Soc. Lond. A, 297, 605, 1980.

Montgomery, M. D., J. R. Asbridge, S. J. Bame, W. C. Feldman, Solar wind electron depressions following some interplanetary shock waves: Evidence for magnetic merging?, J. Geophys. Res., 79, 3103, 1974.

Morrison, P., Solar-connected variations of the cosmic rays, Phy. Rev., 95, 641, 1954.

Mouschovias, T. C., A. I. Poland, Expansion and broadening of coronal loop transients: A theoretical explanation, Astrophys. J., 220F, 675, 1978.

Palmer, I. D., F. R. Allum, and S. Singer, Bidirectional anisotropies in solar cosmic ray events: Evidence for magnetic bottles, J. Geophys. Res., 83, 75, 1978.

Parker, E. N., The gross dynamics of a hydromagnetic gas cloud, Ap. J., Supplement, No. 25, p. 51, 1957.

Piddington, J. R., Interplanetary magnetic field and its control of cosmic-ray variations, Phys. Rev., 119, 589, 1958.

Pneuman, G. W., Eruptive prominences and coronal transients, Solar Phys., 65, 369, 1980.

Pneuman, G. W., Reconnection and coronal transients, to appear in Proc. IAU Symposium No. 91: Solar and Interplanetary Dynamics, August 27-31, 1979, Cambridge, Mass., 1981.

Poland, A. I., R. A. Howard, M. J. Koomen, D. J. Michels, and N. R. Sheeley, Jr., Coronal transients near sunspot maximum, Solar Phys., in press, 1980.

Pudovkin, M. I., S. A. Zaitseva, L. P. Oleferewko, A. D. Chertkov, The structure of the solar flare stream magnetic field, Solar Phys., 54, 155, 1977.

Pudovkin, M. I., S. A. Zaitseva, E. E. Bewevolewska, The structure and parameters of flare streams, J. Geophys. Res., 84, 6649, 1979.

Rosenberg, R. L., P. J. Coleman, Solar-cycle dependent North-South field variations in solar wind interation regions, J. Geophys. Res., 85, 3021, 1980.

Rust, D. M., E. Hildner, M. Dryer, R. T. Hansen, A N. McClymont, S. M. P. McKenna-Lawlor, P. J. McLean, E. Schmahl, R. S. Steinolfson, E. Tandberg-Hanssen, R. Tousey, D. Webb, and S. T. Wu, In Solar Flares, A Monograph from Skylab Solar Workshop II (ed. P. Sturrock), p. 273, Boulder: University of Colorado Press, 1979.

Schatten, K. H., N. F. Ness and J. M. Wilcox, Influence of a solar active region on the interplanetary magnetic field, Solar Phys., 5, 240, 1968.

Sonnerup, B. U. O., L. J. Cahill, Magnetopause structure and attitude from Explorer 12 observations, J. Geophys. Res., 72, 171, 1967.

TABLE 1(a)

Magnetic Cloud following a Shock

Start (YR-DAY-HR)	Stop (YR-DAY-HR)	λ_2/λ_3	β	θ	ϕ
67 - 12-21	67 - 14-07	9.9	91	24	195
67 - 363-15	68 - 0-09	29.0	99	21	177
68 - 26-09	68 - 27-06	4.8	46	2	106
69 - 237-12	69 - 238-06	21.0	102	19	195
72 - 20-03	77 - 21-00	2.5	72	33	216
72 - 32-05	72 - 33-19	15.0	79	30	214
72 - 81-03	72 - 81-18	2.9	138	24	137
72 - 305-02	72 - 306-00	15.5	72	19	196
73 - 102-00	73 - 103-04	3.2	106	-27	144
73 - 140-04	73 - 140-21	1.9	119	43	165
74 - 284-12	74 - 285-22	2.9	88	5	170
78 - 3-10	78 - 4-20	2.3	70	14	240
78 - 92-18	78 - 93-15	4.9	82	1	204

TABLE 1(b)

Magnetic Cloud Preceding an Interaction Region

Start (YR-DAY-HR)	Stop (YR-DAY-HR)	λ_2/λ_3	β	θ	ϕ
68 - 57-18	68 - 58-12	6.4	111	22	169
68 - 176-18	68 - 177-11	5.3	78	2	190
69 - 22-18	69 - 23-21	4.4	62	14	201
71 - 97-10	71 - 98-03	3.2	46	-32	180
72 - 14-12	72 - 15-01	13.8	37	-8	180
72 - 40-03	72 - 40-21	8.4	55	29	213
73 - 19-11	73 - 20-11	6.0	100	46	214
73 - 63-03	73 - 64-03	4.1	111	0	173
73 - 89-21	73 - 91-00	16.6	97	-1	182
73 - 178-20	73 - 179-12	10.8	91	2	231
73 - 206-00	73 - 207-03	6.2	97	43	221
74 - 23-00	74 - 24-06	6.5	90	-8	221
75 - 85-07	75 - 85-22	6.6	74	-45	147
75 - 109-11	75 - 110-07	6.3	107	4	226
76 - 341-06	76 - 342-00	3.3	86	40	217
78 - 51-12	78 - 52-09	16.8	86	-29	214

TABLE 1(c)

Magnetic Cloud Associated with a CME

Start (YR-DAY-HR)	Stop (YR-DAY-HR)	λ_2/λ_3	β	θ	ϕ
67 - 348-21	67 - 350-00	9.9	105	-8	152
68 - 1-03	68 - 002-15	9.7	102	-2	199
69 - 62-18	69 - 63-10	21.0	76	-12	152
71 - 173-14	71 - 175-16	17.5	93	-7	185
72 - 47-06	72 - 48-21	9.0	103	-11	191
72 - 86-17	72 - 87-18	8.8	85	-26	187
72 - 107-21	72 - 108-12	13.5	98	18	174
72 - 331-00	72 - 333-00	4.0	106	-14	117
73 - 268-00	73 - 269-06	15.0	36	1	212
73 - 324-15	73 - 325-05	21.0	89.	-7	160
75 - 144-17	75 - 146-00	5.6	70	-31	206
75 - 212-03	75 - 213-00	17.2	86	-13	171
75 - 320-00	75 - 321-05	11.6	131	-26	164
77 - 155-03	77 - 156-00	4.9	71	-33	208
77 - 268-21	77 - 270-03	16.4	83	-14	184
78 - 15-12	78 - 17-12	6.9	103	34	186

FIGURE CAPTIONS

FIGURE 1   An example of a magnetic cloud preceded by a shock. The cloud boundaries were chosen primarily on the basis of the $\theta(t)$, $T(t)$ and $B(t)$ profiles. The hodograms on the right are projections of B on the plane of maximum variance (X-Y plane) and on the Z-Y plane, where Z is the minimum variance direction and X is the maximum variance direction. The angles θ and ϕ in the figure on the left are the solar ecliptic latitude and longitude, respectively. The numbers on the bottom right give the ratio of the intermediate to maximum eigenvalue (λ_2/λ_3) and the minimum variance direction (θ_n, ϕ_n).

FIGURE 2   A magnetic cloud followed by a stream interface and a sector boundary.

FIGURE 3   A magnetic cloud associated with a CME (a cold region in which the magnetic field strength is enhanced).

FIGURE 4   A magnetic cloud associated with a CME and a sector boundary.

FIGURE 5   The minimum variance directions for the three classes of clouds, in solar ecliptic coordinates. The number of events in each category is N.

FIGURE 6   A superposed epoch analysis of the field strength and the magnitude of θ. The results were obtained by aligning the front boundaries of the clouds (time zero) and averaging successive 6-hour intervals in the time series. The error bars are errors in the mean, (RMS/ N). The rear boundaries are only approximate.

FIGURE 7   A superposed epoch analysis of the speed, density and temperature.

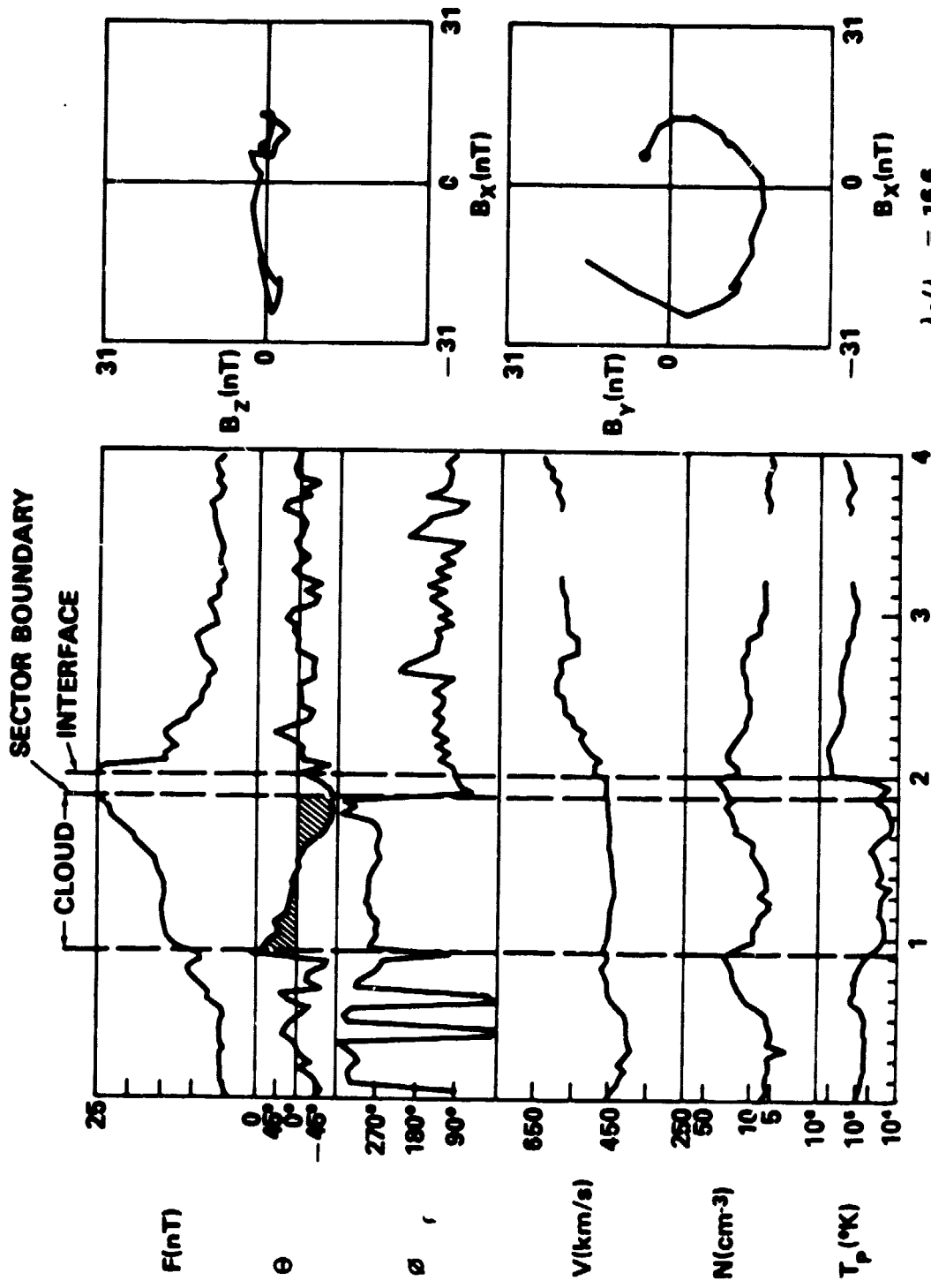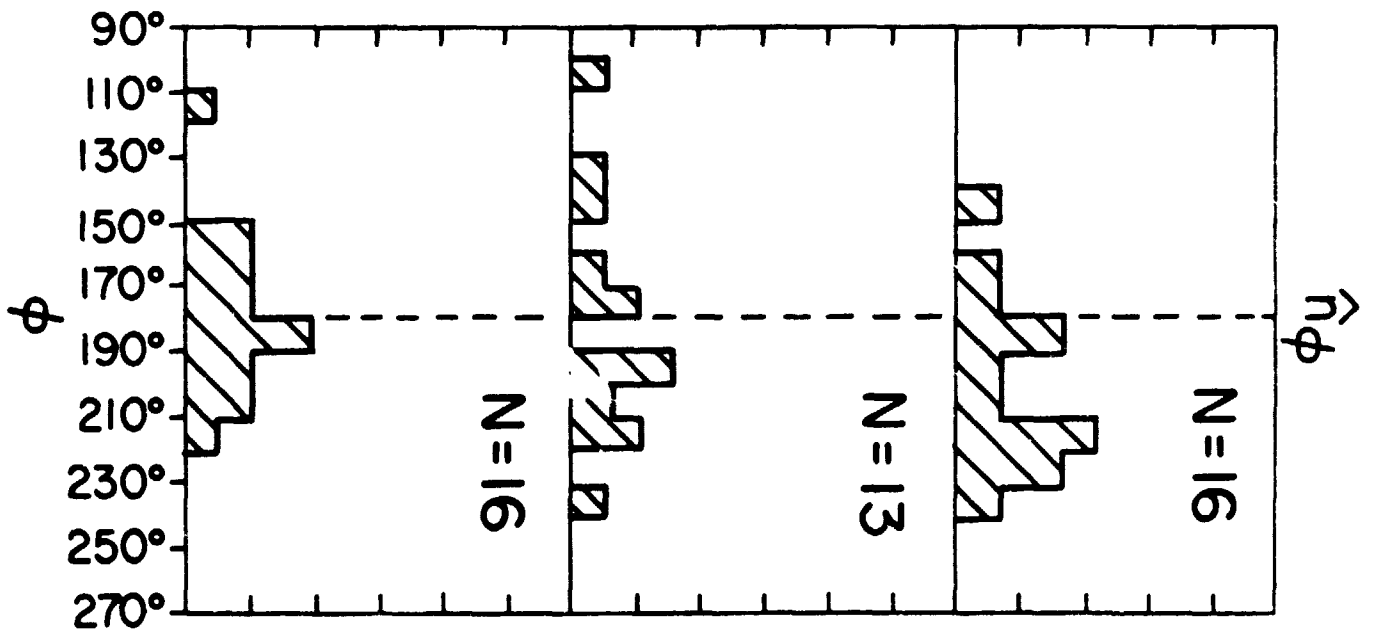FIGURE 8   A superposed epoch analysis of β, the total pressure and the momentum flux.
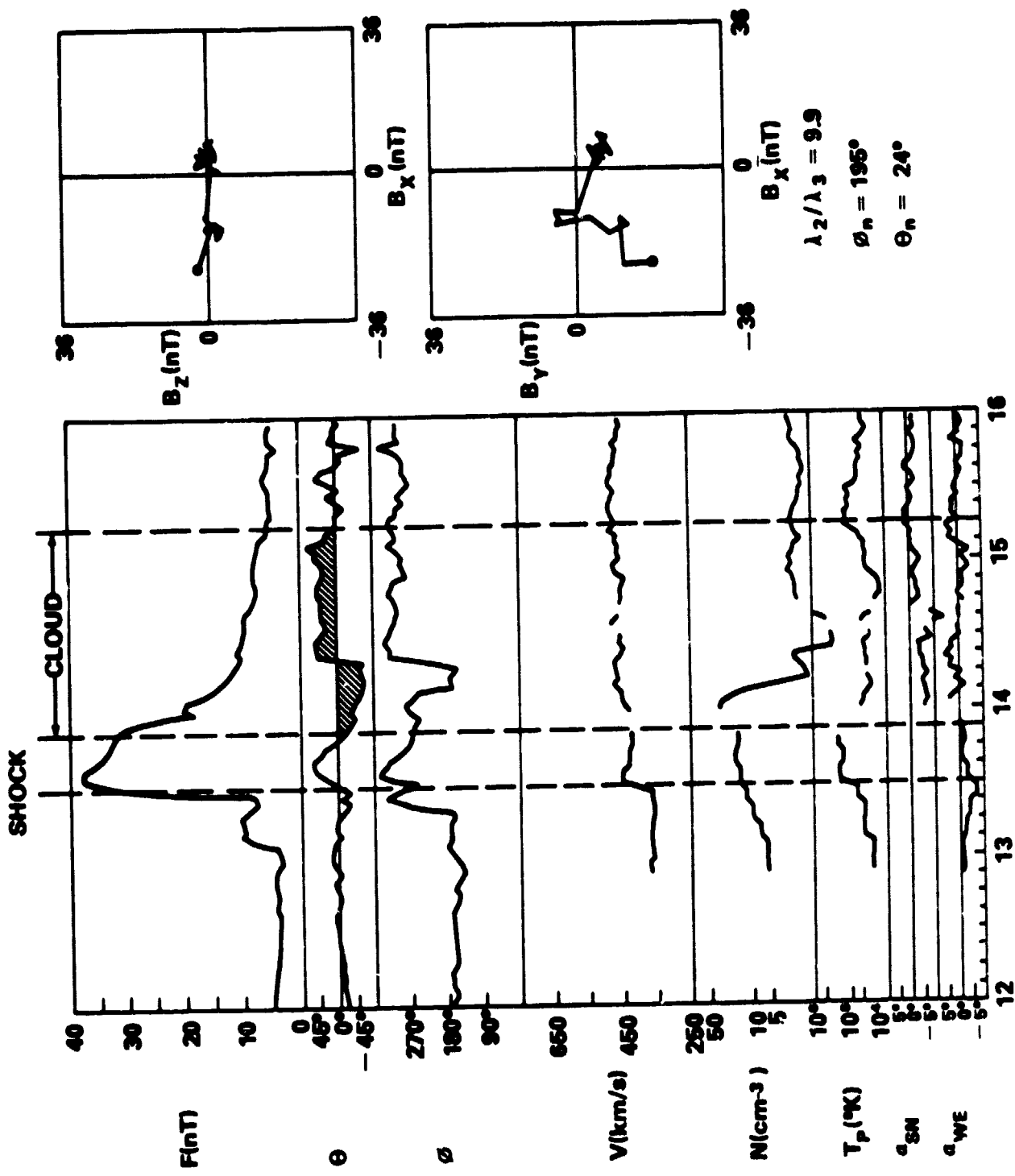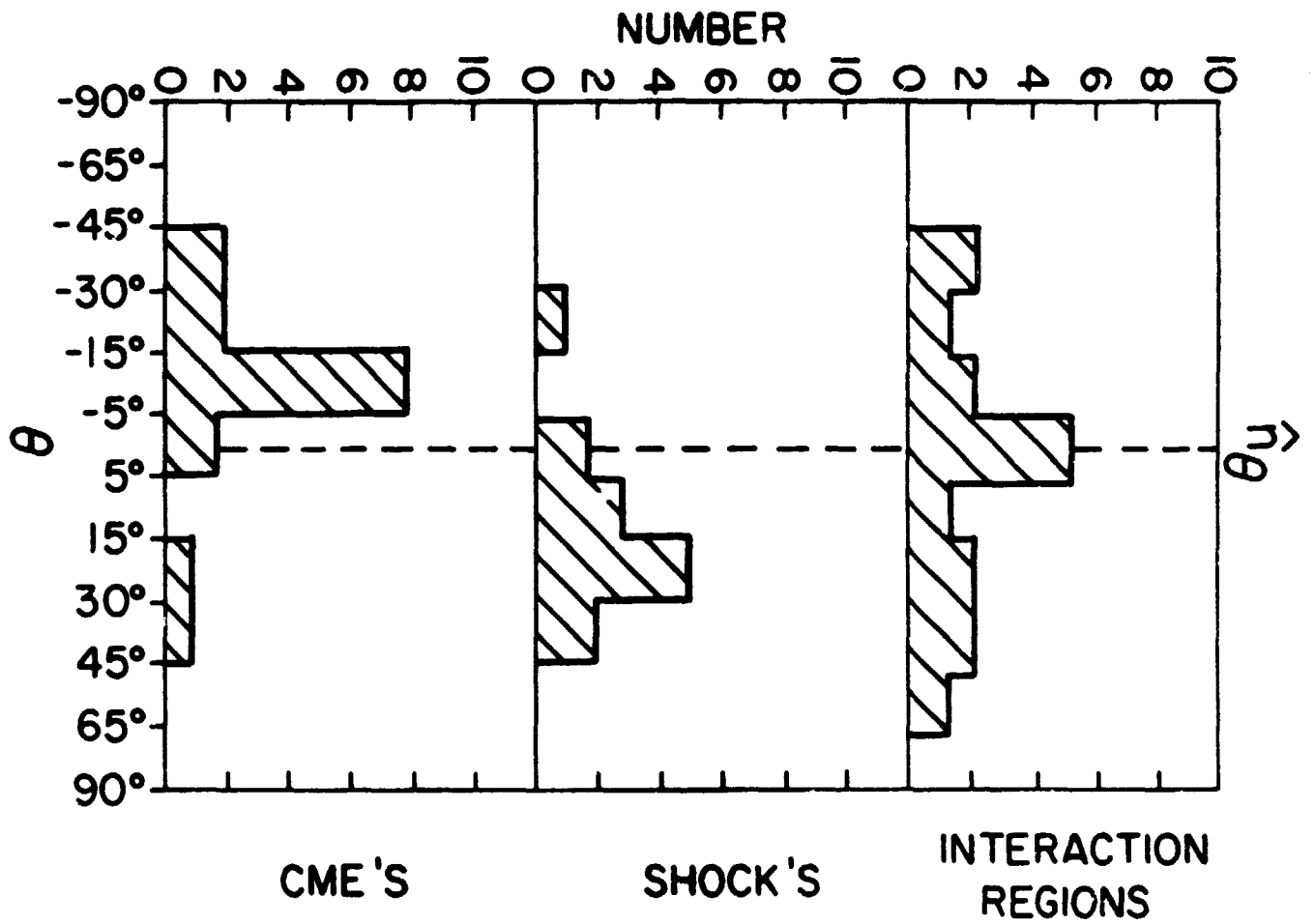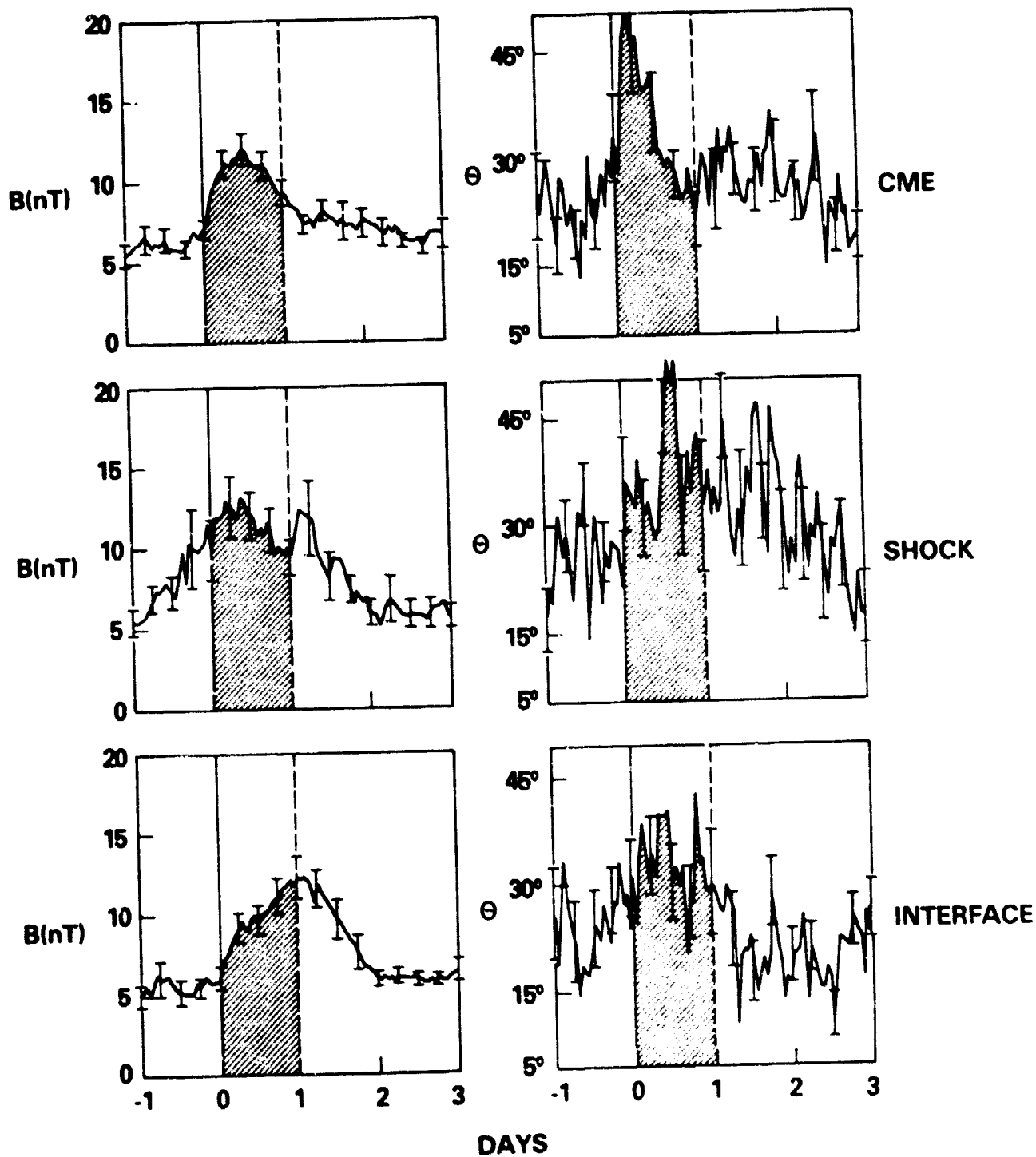
Figure 1
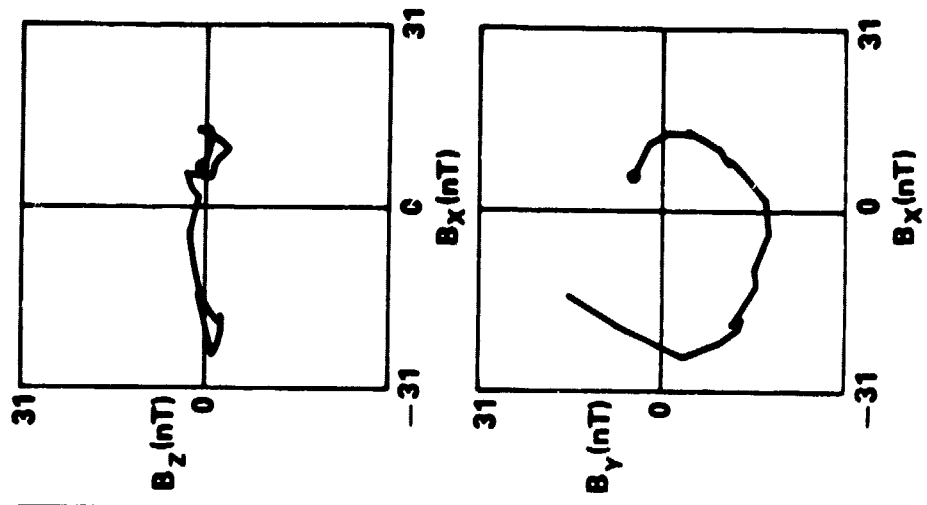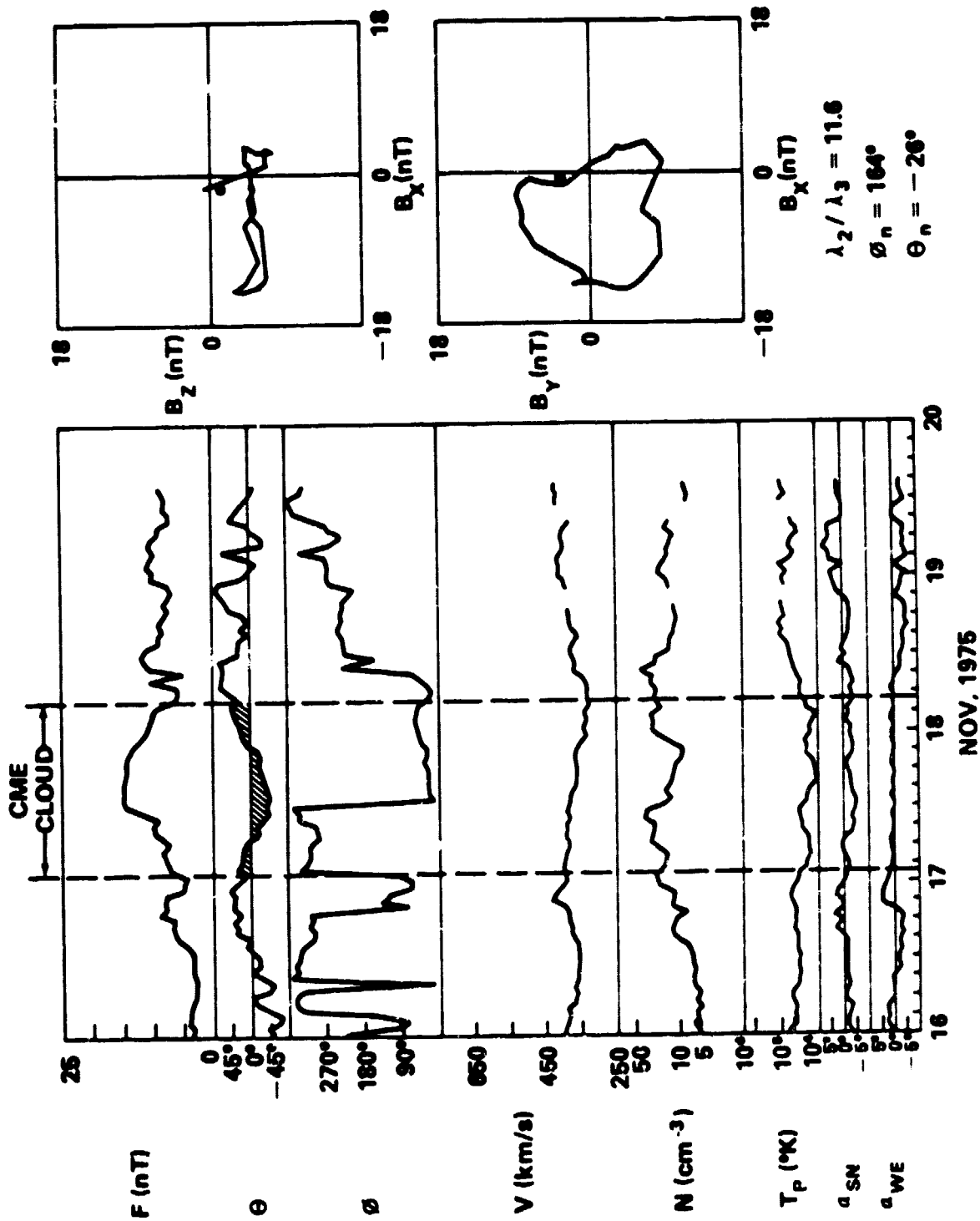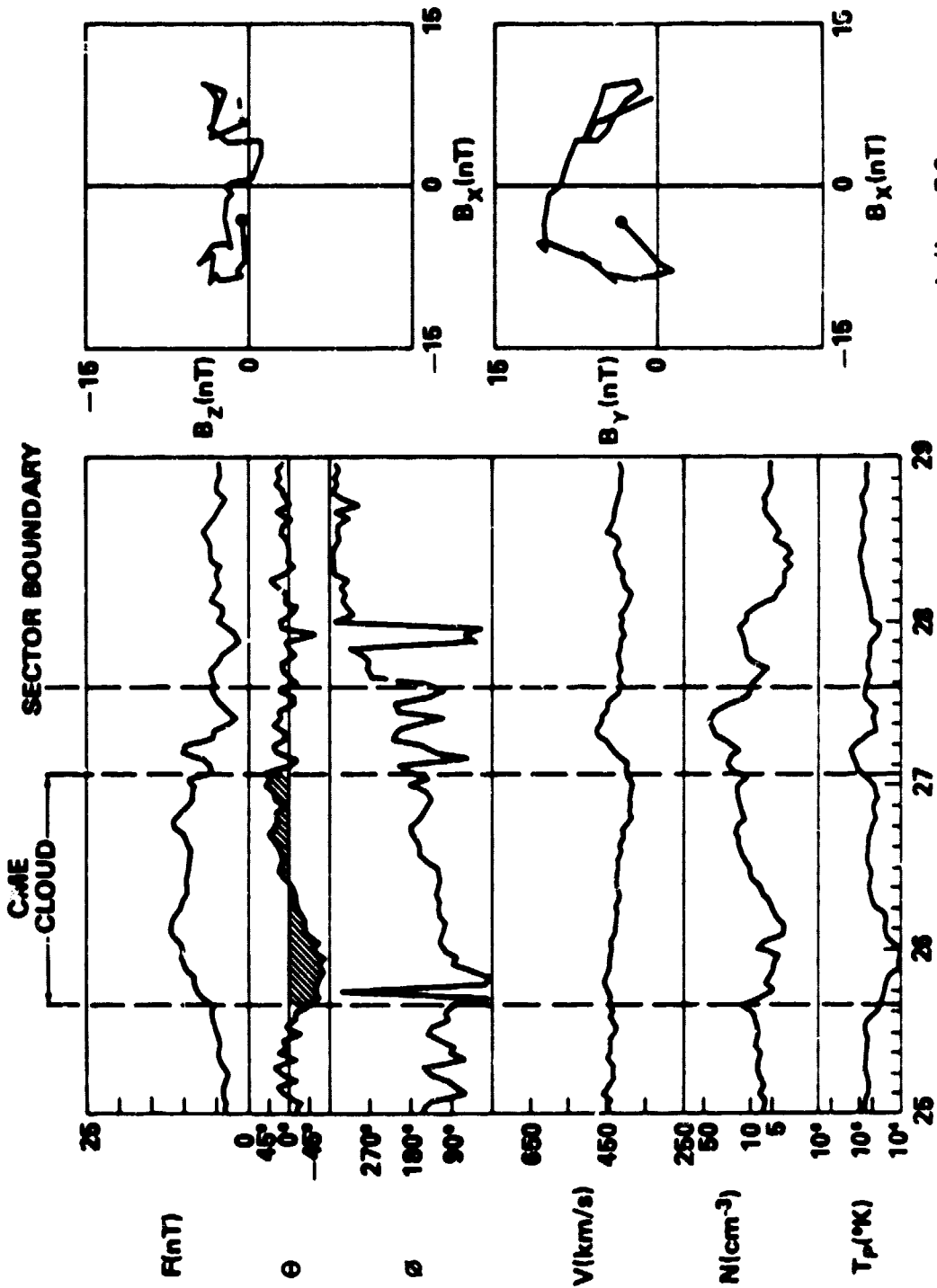
Figure 2

Figure 3

Figure 4

Figure 5

Figure 6

Figure 7

Figure 8